iScience

CellPress
OPEN ACCESS

Article

# Phase-change materials reinforced intelligent paint for efficient daytime radiative cooling

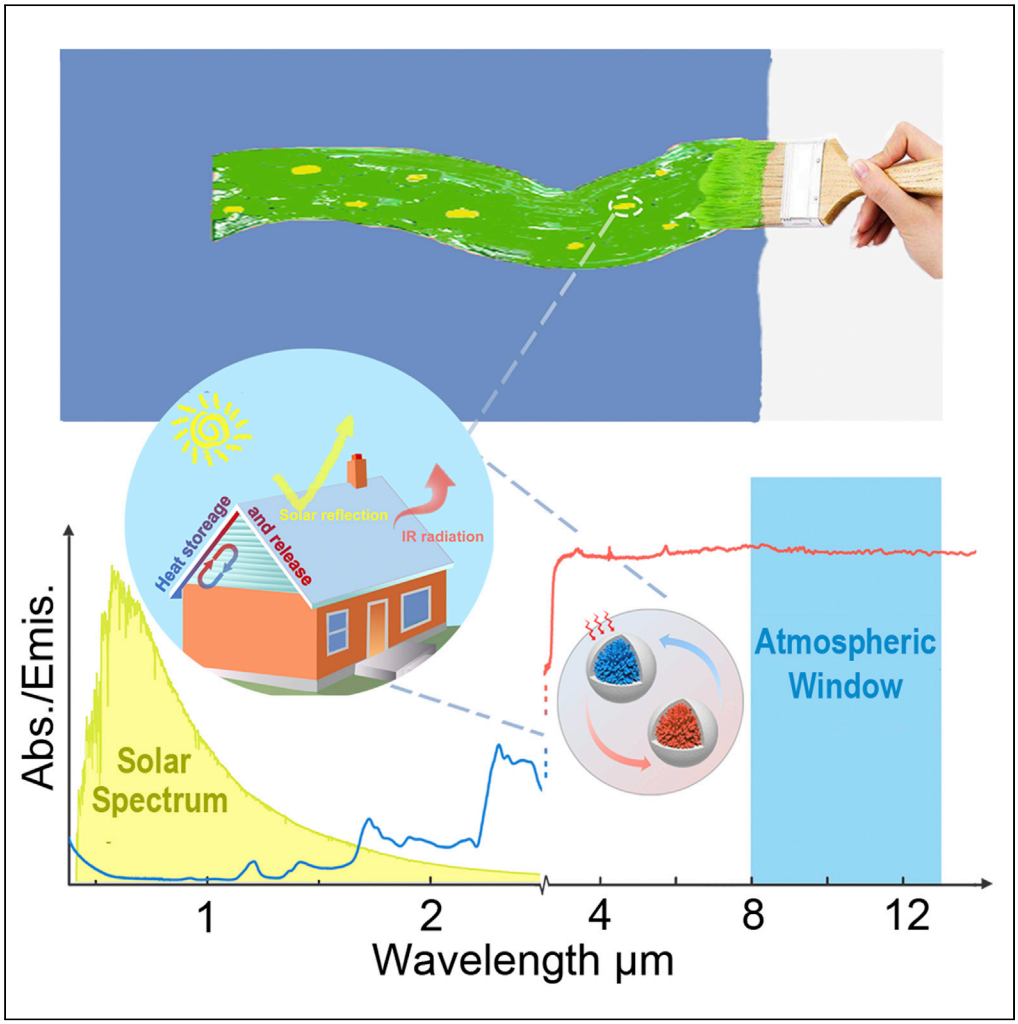


Mulin Qin, Feng Xiong, Waseem Aftab, Jinming Shi, Haiwei Han, Ruqiang Zou

rzou@pku.edu.cn

## Highlights

Bifunctional paint with radiative cooling and latent heat abilities was developed

Phase-Change Materials used for isothermal storage of importing heat

High reflectivity of paint derived from micro size distribution of the microcapsules

Temperature drop and time buffering effect was achieved by bifunctional paint

Qin et al., iScience 25, 104584
July 15, 2022 
https://doi.org/10.1016/j.isci.2022.104584

iScience

CellPress
OPEN ACCESS

Article

# Phase-change materials reinforced intelligent paint for efficient daytime radiative cooling

Mulin Qin,[1,3] Feng Xiong,[1,3] Waseem Aftab,[1,3] Jinming Shi,[1] Haiwei Han,[1] and Ruqiang Zou[1,2,4,*]

## SUMMARY

**Passive cooling of buildings has become increasingly important for green and low-carbon development, especially in the near decade where daytime radiative cooling technology (DRCT) has drawn attention with big breakthroughs. However, irresistibly importing heat from sunlight and surroundings results in notable temperature rise, thus limiting the cooling effect. Here, we report a radiative paint with latent heat storage capacity to store imported heat by coupling randomly-distributed phase-change materials (PCMs) based microcapsules with acrylic resin to enhance cooling performance. The bifunctional paint shows good performance in selected-suitable phase transition temperature, high enthalpy, high reflectivity in the sunlight region and strong emissivity in the atmospheric window region. The temperature measurements demonstrate that the paint possesses enhanced cooling performance of temperature drop and time buffering effect compared with the pure radiative cooling paint. This work offers the potential to broaden the applications of PCMs and DRCT for energy saving and environment protection.**

## INTRODUCTION

Space cooling systems depending on modern refrigeration techniques such as air conditioning and ventilation with low energy efficiency dramatically result in large energy consumption and massive greenhouse gas emissions (Cai et al., 2009; D'Oca et al., 2018; Pakdel et al., 2019). The proposal of passive thermal management systems without energy consumption is of great significance to alleviate this situation (Rotzetter et al., 2012; Hsu et al., 2016). Daytime radiative cooling technology as one of the most efficient passive-cooling strategies has gained tremendous attention recently, which takes advantage of the enhanced IR emission of heat passing through the atmospheric window into deep space without energy consumption (Raman et al., 2014). To achieve high cooling performance, the ideal radiative coolers should combine both the materials selection and structural design to satisfy the following requirements (Raman et al., 2014; Hossain and Gu, 2016): (1) high emissivity located at 8–13 μm IR region in which there is nearly no IR absorption by air, (2) high solar reflectivity to decrease the solar energy absorption, and (3) avoided surrounding heat input weakening the cooling effect.

Based on these principles, years of researches and efforts have verified excellent cooling performance of DRCT from 2014 (Raman et al., 2014; Zhai et al., 2017; Mandal et al., 2018; Li et al., 2019, 2021; Wang et al., 2021; Zeng et al., 2021). Raman et al. report a photonic radiative coolers composed of seven varying-thickness alternant layers of $HfO_2$ and $SiO_2$ that exhibited high sunlight reflectance of 97% and high selective emissivity in the atmospheric transparency window, and the former was achieved by combining material property of $HfO_2$ being in high-index material and interference effects of periodic one-dimensional photonic crystals, the latter by strong absorption of $SiO_2$ located around 9.5 μm deriving from Si-O-Si resonance (Raman et al., 2014). With optimized design, the coolers obtained an efficient cooling effect of 4.9°C lower than ambient temperature when exposed to direct sunlight. For large-scale manufacture, the radiative coolers such as randomized $SiO_2$-polymer hybrid metamaterial (Zhai et al., 2017), hierarchically porous polymer coatings (Mandal et al., 2018), hierarchically designed polymer film (Wang et al., 2021), etc. are reported recently, and the shown optimizing works of high solar reflectivity and high IR emissivity are done by evaluating their sub-ambient cooling effect on the surface of well-thermal-insulated boxes. Further, eliminating the input of surrounding heat and other parasitic heat is of apparent significance to enhance the cooling efficiency for radiative cooling systems. Therefore, a low thermal-conductivity matrix

[1]Beijing Key Laboratory for Theory and Technology of Advanced Battery Materials, School of Materials Science and Engineering, Peking University, Beijing 100871, P. R. China

[2]Institute of Clean Energy, Peking University, Beijing, P. R. China

[3]These authors contributed equally

[4]Lead contact

*Correspondence: rzou@pku.edu.cn

https://doi.org/10.1016/j.isci.2022.104584

(Zhong et al., 2021) and an accessorial thermal-insulation layer (Leroy et al., 2019) are proposed as effective strategies to establish thermal resistance dealing with the parasitic heat.

Despite lots of efforts focusing on stringent high reflectivity and strong IR emissivity design for the radiative coolers, and even on the thermal-insulation layer establishing, the parasitic heat from all surroundings will be imported irresistibly accompanied by notable temperature increase and cooling effect reduction. Thus, if there is a heat container incorporated to store the invasive thermal energy, the DRCT systems can predictably achieve a better cooling effect. In this regard, phase-change materials (PCMs) can be the ideal choice considering its merit of the high thermal capacity when going through an isothermal phase transition and has been deeply explored in the field of building thermal management for buffering temperature in repaid variation (Aftab et al., 2018, 2021; Yuan et al., 2019; Shi et al., 2020, 2021; Akeiber et al., 2016; Zhou et al., 2012). PCMs include varieties of organic, inorganic, and composite materials with the advantages of wide temperature selectivity and high energy storage density (Pielichowska and Pielichowski, 2014). These features endow PCMs with great potentials as irresistible heat containers for the radiative coolers. However, the usage of PCMs is severely limited by leakage problems in the liquid state (Aftab et al., 2018; Shchukina et al., 2018). Meanwhile, the incorporation of PCMs should avert a negative effect on the radiative cooling capacity of the original coolers. Preparations to meet all the requirements seem to be a great challenge, and effective research about PCMs-based radiative coolers is still absent in the literature.

In this work, we design a bifunctional paint by adopting radiative paint with latent heat storage capacity for enhanced cooling performance. By simply mixing microcapsule particles and acrylic resin, the paint is prepared scalably. Its high solar reflectivity results from the presence of microcapsules with distributed diameters ranging in 0.5–1.5 μm triggering a strong Mie scattering effect to reflect sunlight (Li et al., 2021; Zeng et al., 2021; Zhou et al., 2021), and the high IR emissivity derives from the abundant vibration of Si-O-Si, C-O bonds located at atmospheric window (Zhai et al., 2017; Li et al., 2020, 2021; Jaramillo-Fernandez et al., 2019). By optimizing the materials selection and structure design, the paint is demonstrated to simultaneously own the solar-spectrum average reflectivity of 95.6% and the average mid-IR emissivity of 95.95% in an 8–13 μm region. The as-prepared paint shows a suitable phase transition temperature of 28–34°C and high enthalpy of 71.35 J/g to meet the requirement of heat storage as well as daytime radiative cooling. The functional role of PCMs can be described as an invasive heat container for the cooling procedure owing to the constant-temperature property during phase transition. The cooling performance test shows that our bifunctional paint can achieve more temperature drop and time buffering effect compared with the homemade $SiO_2$-particle based radiative paint. Given the enhanced cooling effect, the incorporation of latent heat storage capacity into radiative paint verified that it will offer the opportunity to broaden the applications of PCMs and DRCT.

## RESULTS

The bifunctional paint for efficient cooling is schematically shown in Figure 1A. It consists of thermoplastic acrylic resin as radiative binder and randomly distributed $SiO_2$-PCMs microcapsules as solar-light strongly scattered particles, heat containers, and additional IR emitters. The intrinsically high-emissivity acrylic resin with the existence of resonance mode of C-O bond located at the atmospheric window is commercially available (Figure S2). Meanwhile, $SiO_2$ with the strong phonon-polariton resonances at 9.7 μm to strongly emit mid-IR is used for encapsulating PCMs to solve its leakage drawback in the liquid state. Microencapsulation is a general method to confine PCMs in nano-micro scale, and by engineering its size distribution ranging in solar spectral scale, the PCMs-based microcapsules can exhibit high enough sunlight reflectance. Figure 1B shows the computational scattering efficiency of the solar spectrum as a function of diameters by using FDTD solution software (Figure S3), and it is corroborated that core-shell structural particles with the diameters distributed in the 500–1,500 nm can strongly scatter the sunlight within the full spectrum. Eventually, based on the controllable optical and thermal properties, the combination of acrylic resin and PCMs microcapsules can achieve radiative cooling and constant temperature heat storage capacities to enhance the total cooling effect.

To obtain the designed size distribution of microcapsules, a modified interfacial hydrolysis and polycondensation method of the microemulsion is developed (synthesis details in STAR Methods) (Liang et al., 2015). A smaller ratio between deionized water and ethanol is conducive to forming a higher volume of microemulsion and obtaining a larger diameter distribution. Figures 1C and 1D and F–I show the SEM image

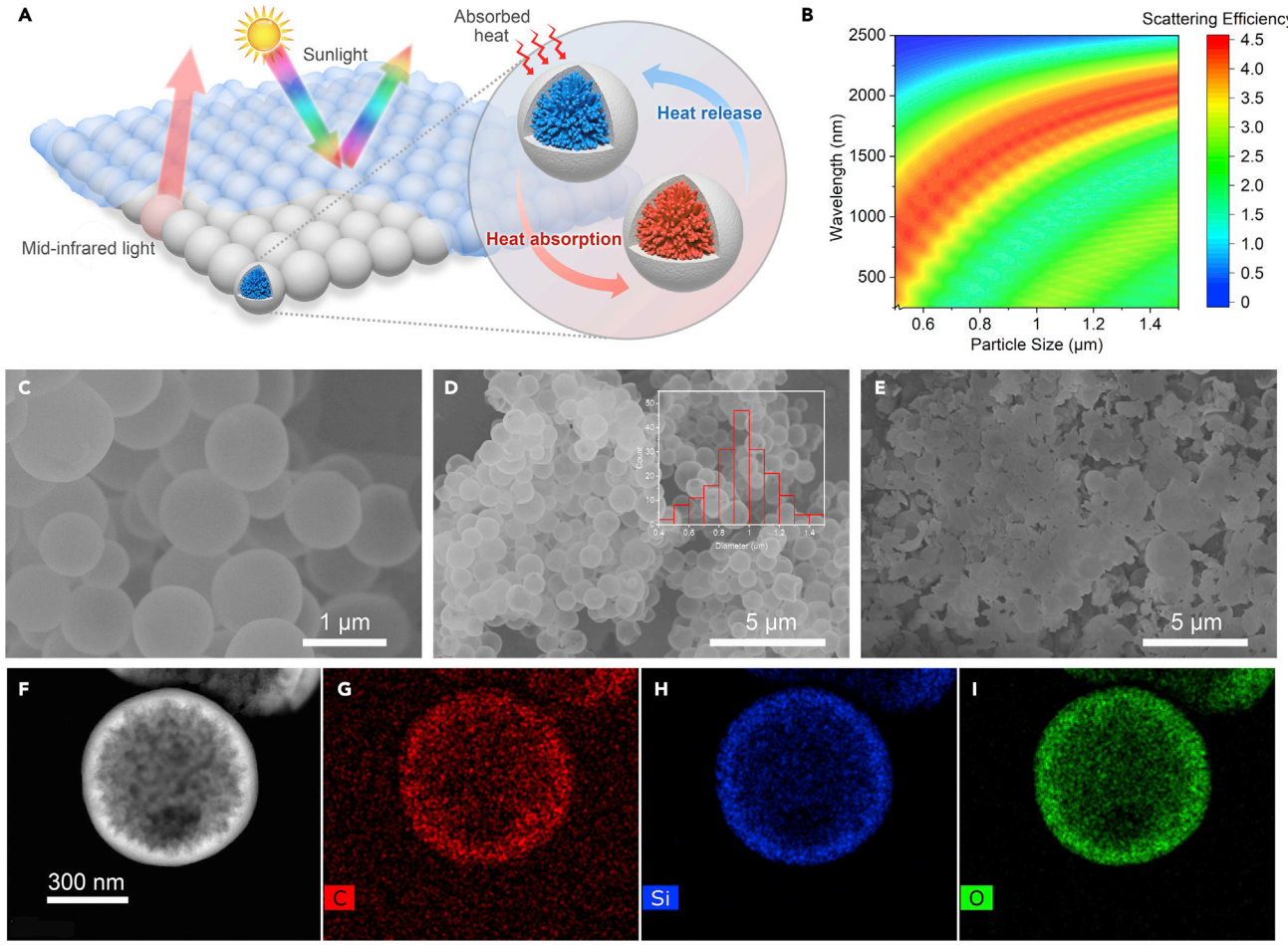


**Figure 1. The theoretical analysis and structure properties of bifunctional paint**

(A) The schematic diagram of the paint design which consists of thermoplastic acrylic resin and randomly distributed $SiO_2$-PCMs microcapsule. The sunlight is reflected by the micro size distributed microcapsules, and the IR emission is responded with high emissivity polymer and $SiO_2$ shell, and irresistibly importing heat is stored by phase transition of PCMs.

(B) Simulated scattering efficiency of the microcapsule over the wavelength range of 300–2500 nm with the particle diameter varied from 0.5 to 1.5 μm.

(C and D) The SEM image of microcapsules. Inset: the diameter distribution of the microcapsules.

(E) The SEM image of bifunctional paint.

(F–I) The TEM image and element mapping of the single microcapsule.

and TEM image of the as-prepared microcapsules. The samples are presented as completed core-shell structures especially for the particles whose diameters are lower than 1 μm. The particle sizes are mainly distributed in the 0.5–1.5 μm range, which is comparable to the wavelengths of ultraviolet, visible, and near-IR lights to satisfy high scattering efficiency requirements and induce strong Mie scattering effects. The paint is prepared by an accessible mixed process of microcapsules and acrylic resin and follows natural drying after painting to avoid surface cracking. To increase the loading percentage of PCMs in the paint to store more imported heat while avoiding its surface crack, we optimized the ratio between microcapsules and acrylic resin, and 7:3 turns out to be an appropriate choice. The SEM image of the paint is shown in Figure 1E, in which the main microcapsules stay in the original spheroidal morphology. Taking advantage of this insight structure, the paint appears in white color (Figure S4).

To evaluate the radiative cooling capacity of the paint, we experimentally measure its optical properties. The microcapsules are pressed into the tablet shape forming a smooth surface with the assistance of pressed cracked particles and leaked paraffin, and then the tablet is used to test the optical constant. The real and imaginary parts of the effective refractive index, namely refractive index ($n$) and extinction coefficient ($k$), as a function of wavelength are illustrated in Figures 2A and 2B. The former index refers to the

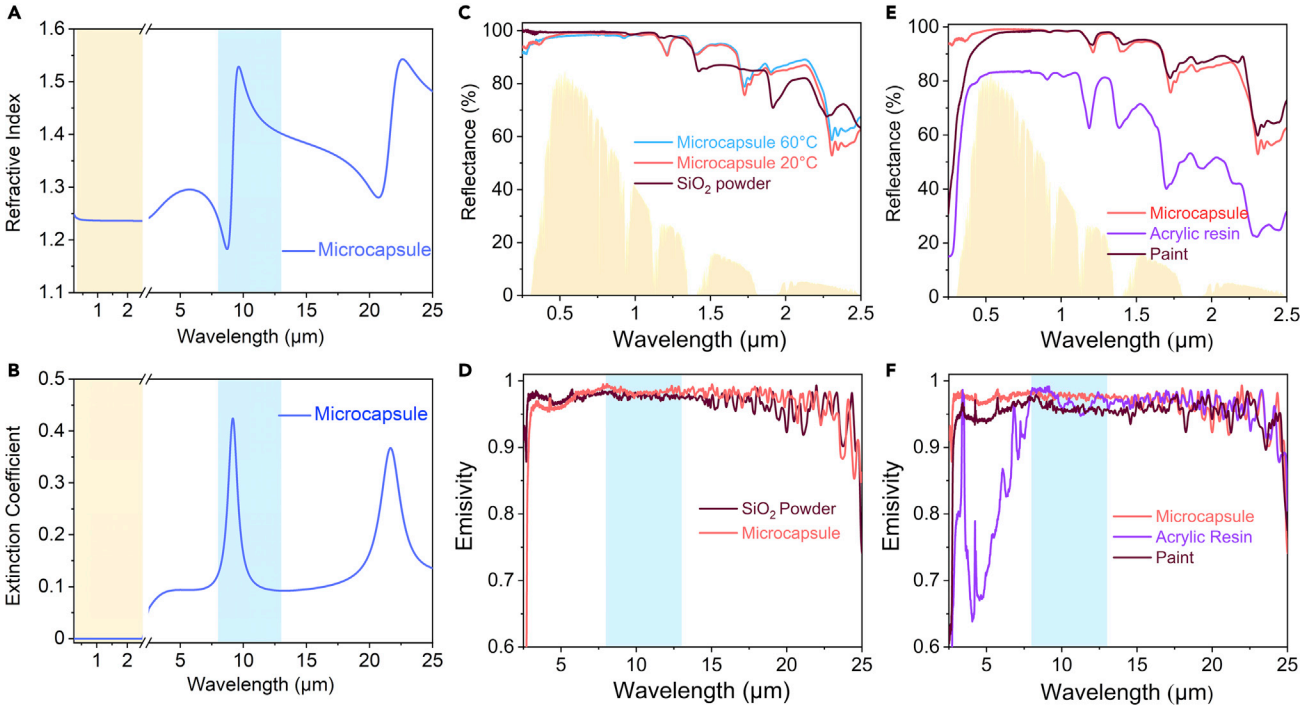


**Figure 2. The optical properties of the bifunctional paint**

(A and B) The real and imaginary part of the effective refractive index of microcapsule tablet. There is a strong phonon-polariton Fröhlich resonance located at the atmospheric window.

(C and D) the reflectivity and emissivity spectrum of the microcapsule and $SiO_2$ microsphere powder.

(E and F) the reflectivity and emissivity spectrum of the composite paint. The yellow and blue fill refer to the sunlight region and atmosphere window region, respectively.

ratio of light speed in the vacuum and medium and a higher value means higher reflectance according to the equation of $R = [(n-1)^2 + k^2]/[(n+1)^2 + k^2]$, and the latter refers to the absorption of light by the medium, and a higher value means higher absorbance. In the sunlight region, the refractive index in the value of 1.24 for the microcapsules is obtained but is lower than normal $SiO_2$ and paraffin because of the amorphous $SiO_2$ shell (XRD pattern in Figure S5) and air filling between the particles. Meanwhile, the close-to-zero extinction coefficient verifies that the microcapsules have negligible absorption over the entire sunlight range. The strong phonon-polariton Fröhlich resonance peak (around 9.2 μm) is obtained and located at the atmospheric window, which explains the high IR absorption in this region (Zhai et al., 2017). The temperature-dependent reflectivity of the microcapsules shown in Figure 2C is 96.66% at 20°C and 96.92% at 60°C. The negligible difference before and after the phase transition is because of the coating effect of the microcapsules, which cut off the influence from inside phase transition. It is worth mentioning that the high reflectance can be achieved deriving from the particles' Mie scattering effect even in lower refractive index. The reflectance of $SiO_2$ microsphere powder is measured at the value of 97.41%, which is used for the construction of pure radiative cooling paint. Figure 2D shows that microcapsules and $SiO_2$ powders own similar broadband high emissivity in 2.5–25 μm, and in the 8–13 μm range, these are 98.42%, 97.57% in average, respectively. The sunlight reflectance and IR emissivity of paint are tested as illustrated in Figures 2E and 2F. With microcapsules, the sunlight reflectance of the composite paint (in the thickness of around 600 μm) is greatly enhanced from 78.28% to 95.6% compared with original acrylic resin, slightly lower than pure microcapsules. There is high absorption in the ultraviolet for the acrylic resin region but mitigated for the composite paint because of the existence of strong particle scattering. Meanwhile, the paint exhibited similar high broadband emissivity like the microcapsules and the average emissivity in the 8–13 μm region is 95.95%. Eventually, the conducted optic tests demonstrate that phase-change microcapsules incorporated paint exhibit the optimized radiative capacity with high sunlight reflectance and high atmospheric windowed emissivity, which can meet the requirement of the radiative cooling applications.

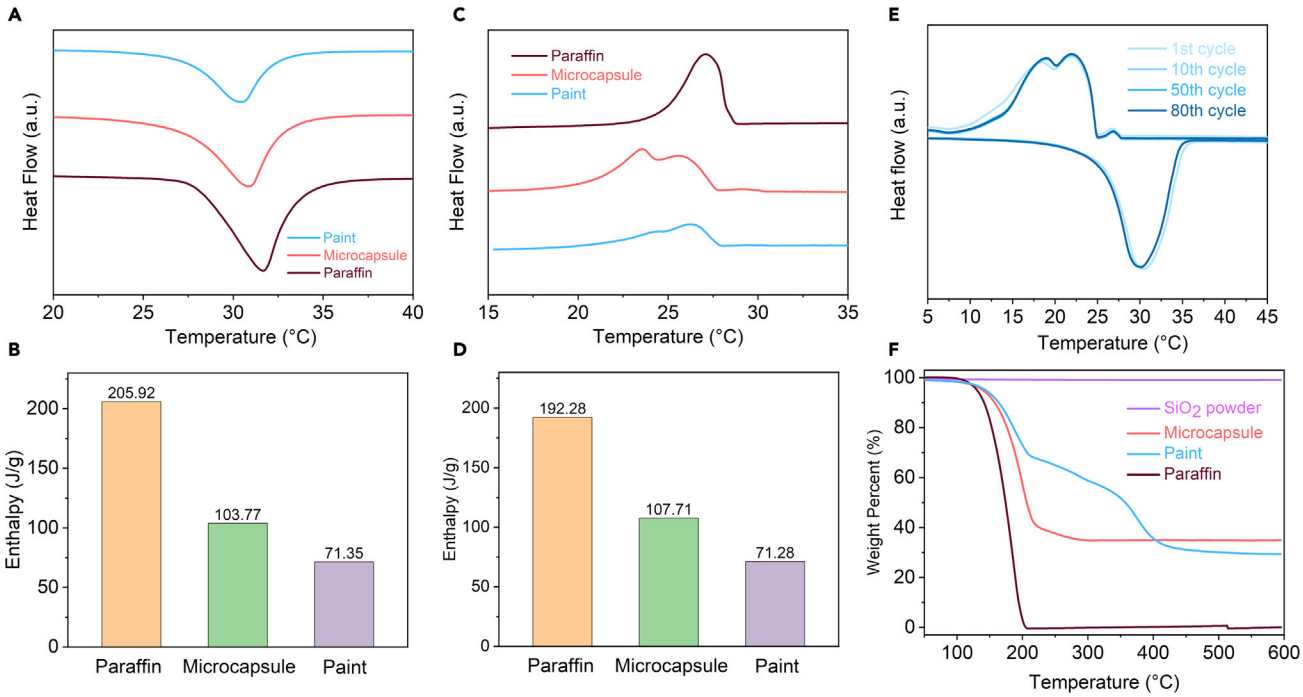


**Figure. 3. Thermal properties of the bifunctional paint**

(A and C) The DSC heating and cooling curve of the original paraffin, microcapsules, and paint, respectively.

(B and D) the corresponding melting and freezing enthalpy of paraffin, microcapsules, and paint, respectively.

(E) Thermal cycling performance of the microcapsules.

(F) TGA curve of the $SiO_2$ powder, microcapsules, paraffin, and paint.

To store the importing heat from sunlight and surrounding, the phase-change medium is chosen to meet the temperature requirement. PCMs can be selected with variable melting temperatures according to different regions and weathers, because they are convertible. Considering the maximum ambient temperature that is higher than 32°C on a general Beijing summer day and the radiative cooling effect, octadecane is chosen as the phase change medium whose melting temperature is 28–34°C. The phase-change behavior that plays an important role in this bifunctional paint is investigated using differential scanning calorimetry (DSC). Figures 3A–3C show the heating and cooling DSC curves of octadecane, microcapsules and paint, and their corresponding data are presented in Figures 3B and 3D. The melting temperature of microcapsules and paint has slight variation compared with the original paraffin, which will not impact function implementation of heat storage when used as the heat container. The cooling curve shows that the crystallization temperature of the paint is 27.8–20.5°C same with the microcapsules but slightly lower than the original paraffin, which is attributed to the geometric constraint effect of the micro-shell. The appearing two main peaks with temperature decreasing in the cooling curve of the microcapsules refer to the two-step transformation from liquid to the metastable rotator phase and from rotator phase to stable triclinic crystal phase, respectively (Liang et al., 2015). For a one-day cycle, the heat will be absorbed in the daytime when the temperature is up to the melting point and released at nighttime when down to the cooling point, and the former will boost the cooling effect but the latter will weaken heat dissipation. It is worth mentioning that the released heat will not give much passive effect to the all-day cooling because of the elimination of sunlight power at night. On the other hand, it will create a more comfortable environment with small temperature difference in the high-temperature difference area. The latent heat storage capacity of the paint is 71.35 J/g and the effective mass of crystalline paraffin is 34.70%, exhibiting high thermal density. For practical applications, the more thickness it is, the higher thermal capacity it has. Circulation stable test of the microcapsules is carried out and shown in Figure 3C. All the DSC cycle curves are nearly coincident, demonstrating the stable operation for the microcapsules when going through repeated heating and cooling procedures. The evident small peak (28°C) in the cooling cycle curve refers to the formation of the surface freezing monolayer at the interface between $SiO_2$ shell and octadecane (Liang et al., 2015). Low thermal conductivity is necessary to decrease the import of conductive and

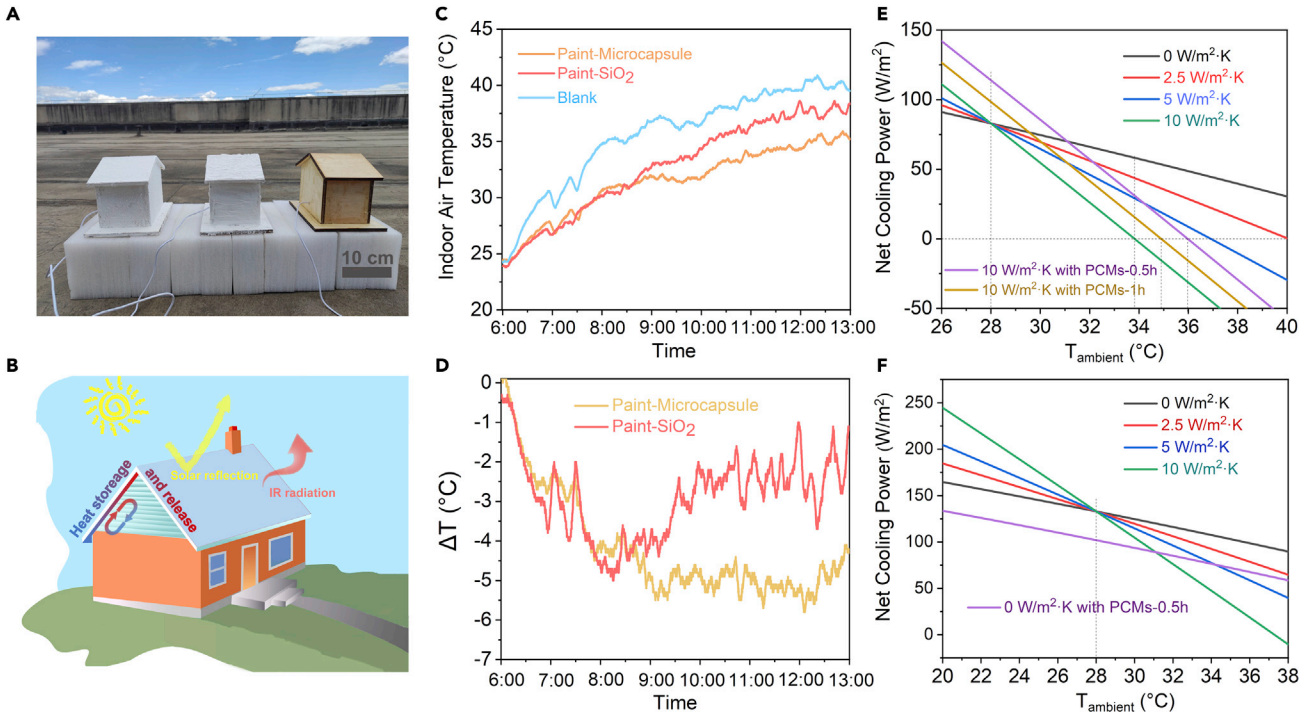


**Figure 4. Cooling performance of the bifunctional paint, in comparison with pure radiative cooling paint and blank**

(A) Set-up of the real-time temperature test for the cooling performance.

(B) Schematic of the setup for testing cooling performance.

(C) Daytime temperatures profiles of indoor air for m-paint, s-paint, and blank house (2nd, August).

(D) Temperature difference of indoor air compared between m-paint and s-paint house with blank, respectively.

(E and F) Calculated net cooling power with ideal PCMs during the phase change procedure in the daytime(E) and nighttime(F).

convective heat for the sub-ambient daytime radiative cooling (Zhong et al., 2021), and that is achieved for the microcapsule in the value of 0.131 W/mK lower than paraffin and $SiO_2$ powder (Figure S6) because of the heterogeneous interfaces introduced inside the particles. Although low thermal conductivity here may reduce the thermal efficiency of PCMs' charging like common issues (Chen et al., 2020; Cheng et al., 2021), as the heat flow in passive cooling systems is relatively low and in turn, the high radiative cooling effect can be achieved. The TGA curves are presented in Figure 3F and illustrate that the paint can maintain stability at the highest temperature of 150°C, whereas paraffin and acrylic resin will decompose successively when heated at 150°C. It is verified that the paint can keep stable for normal room temperature applications. In short, based on the presented thermal properties, the paint with the suitable phase-change temperature and high enthalpy is successfully developed.

## DISCUSSION

To experimentally verify the enhanced cooling effect of the bifunctional paint, we performed a continuous temperature test in Beijing summer days (the weather information is presented in Figure S7). The set-ups are shown in Figures 4A and 4B where the microcapsules incorporated paint (label as m-paint) is brushed at the surface of the homemade wood house model with the average mass densities of 0.08 g/cm$^2$ and 0.06 g/cm$^2$ for the roof and sidewalls, respectively. The radiative paint (labeled as s-paint) composed of $SiO_2$ microsphere and acrylic resin that has similar reflectance in the sunlight region and emissivity in the 8–13 μm range is used as the reference group brushed with the same average mass densities. The original wood house without paint is used as an empty group to silhouette the total cooling effect of the paint. During this test, the houses are exposed directly to circumstances to simulate their practical application and the temperature of the indoor air is recorded. In this setup, we will not minimize the convective/conductive heat transferring from surroundings thus the functional effectiveness of the incorporated PCMs can be verified. Figure 4C shows the indoor temperature profiles of the three houses tested on 2nd, August. In the daytime, the temperature of the house will be going up with the absorption of sunlight radiation and

environmental convective/conductive heat. Because of the radiative cooling capacity, the s-paint house exhibits a slow temperature increase and an average drop of 3°C compared with the blank one. With nearly isothermal heat storage of PCMs, the temperature will go up even more slowly. So the m-paint house exhibits an average temperature drop of 2°C compared with the s-paint house after going through the phase transition from 8:30 to 9:30 (Figure 4D). It is revealed that there is a time buffering effect when incorporating with PCMs that is retard of temperature increased in around 1 h. In the nighttime, the m-paint house shows a higher temperature compared with the other 2 houses because of the heat release, but still, it is in the cooling state (Figure S8). We experiment on another day (22nd September) with lower sunlight power density, and there is an average temperature drop of 1°C for the m-paint house compared with the s-paint house (Figure S9). When the surrounding temperature increases slowly, the buffering effect will be not distinct like the previous test on 2nd, August. Meanwhile, we simplistically calculate the net cooling power with an accepted radiative model[6] to verify the enhanced cooling effect by introducing the phase-change power as the function of ambient temperature with different interface thermal conductivity (Figures 4E and 4F). The net cooling power shows in the value of 82.5 $W/m^2$ in the daytime when the surface temperature equals to ambient temperature, which is comparable to the state-of-the-art radiative cooling materials (Li et al., 2021; Zhou et al., 2021), and with the introduction of PCMs, the value can be increased up to 95–115 $W/m^2$, showing an enhanced cooling performance. It is demonstrated that the existence of PCMs in the radiative cooling systems will increase the surrounding temperature corresponding to the zero net cooling power in the daytime. At the same time, it still maintains the positive value of net cooling power with heat release in the nighttime. In short, all the results demonstrate that bifunctional paint has an enhanced cooling performance as a result of the combination of PCMs and radiative cooling materials.

In conclusion, this work develops a bifunctional paint with both radiative cooling and thermal storage ability for efficient passive cooling by coupling randomly distributed PCMs based microcapsules with acrylic resin. The microcapsules are prepared via surface polymerization process and the paint is prepared through a simple mixed process. It exhibits a high reflectivity in the sunlight region owing to the micro size distribution of the microcapsules, a strong emissivity in the mid-IR region because of the existing vibrations mode, and a suitable phase transition temperature range along with high enthalpy deriving from PCMs. The temperature measurements and power calculations confirm that the bifunctional paint has a temperature drop and time buffering effect compared with the pure radiative cooling paint. Given the enhanced cooling performance, adopting radiative paint with latent heat storage capacity presented here will offer the opportunity for wider applications of PCMs and daytime radiative cooling technologies to reduce the energy dependence of thermal management.

## Limitations of the study

Although the passively cooling performance is enhanced by developing the bifunctional paint with both radiative cooling and thermal storage ability in this work, the temperature still keeps on going up after the phase transition because of the shortage of PCMs and the absorption of the UV light and broad IR. These can be improved by innovative preparations of composite with the properties of high uptake of PCMs, higher sunlight reflectance and selective IR emissivity. Strategies like spinning and layered structure design are recommended for further study.

## STAR★METHODS

Detailed methods are provided in the online version of this paper and include the following:

- KEY RESOURCES TABLE
- RESOURCE AVAILABILITY
  - Lead contact
  - Materials availability
  - Data and code availability
- METHOD DETAILS
  - Sample preparation
  - Morphologies and structure characterization of the microcapsules and paint
  - Optical properties characterization of the microcapsules and paint
  - Thermal properties characterization of the microcapsules and paint
  - The simulation of the scattering efficiency of microcapsule
  - Theoretical simplified model of the enhanced cooling performance

## SUPPLEMENTAL INFORMATION

Supplemental information can be found online at https://doi.org/10.1016/j.isci.2022.104584.

## ACKNOWLEDGMENTS

This work was financially supported by the National Key Research and Development Program of China (2020YFA0210701), the National Natural Science Foundation of China (51825201 and 52102199). The authors acknowledge the Electron Microscopy Laboratory of Peking University, China for the use of Tecnai F30 transmission electron microscopy.

## AUTHOR CONTRIBUTIONS

Conceptualization, M.Q. and W.A.; Methodology, M.Q. and F.X.; Model and Simulation M.Q.; Results' Analysis and Discussion, M.Q., F.X., W.A., R.Z, J.S., and W.H., Writing – Original Draft, M.Q.; Writing – Review & Editing, F.X., R.Z., and J.S.; Visualization, M.Q., F.X., and J.S.; Supervision, R.Z.

## DECLARATION OF INTERESTS

The authors declare no competing interest.

Received: March 28, 2022
Revised: May 15, 2022
Accepted: June 7, 2022
Published: July 15, 2022

## REFERENCES

Aftab, W., Huang, X., Wu, W., Liang, Z., Mahmood, A., and Zou, R. (2018). Nanoconfined phase change materials for thermal energy applications. Energy Environ. Sci. *11*, 1392–1424. https://doi.org/10.1039/c7ee03587j.

Aftab, W., Usman, A., Shi, J., Yuan, K., Qin, M., and Zou, R. (2021). Phase change material-integrated latent heat storage systems for sustainable energy solutions. Energy Environ. Sci. *14*, 4268–4291. https://doi.org/10.1039/d1ee00527h.

Akeiber, H., Nejat, P., Majid, M.Z.A., Wahid, M.A., Jomehzadeh, F., Zeynali Famileh, I., Calautit, J.K., Hughes, B.R., Zaki, S.a.J.R., and Reviews, S.E. (2016). A review on phase change material (PCM) for sustainable passive cooling in building envelopes. Energy Rev. *60*, 1470–1497. https://doi.org/10.1016/j.rser.2016.03.036.

Cai, W.G., Wu, Y., Zhong, Y., and Ren, H. (2009). China building energy consumption: situation, challenges and corresponding measures. Energy Pol. *37*, 2054–2059. https://doi.org/10.1016/j.enpol.2008.11.037.

Chen, X., Gao, H., Tang, Z., Dong, W., Li, A., and Wang, G. (2020). Optimization strategies of composite phase change materials for thermal energy storage, transfer, conversion and utilization. Energy Environ. Sci. *13*, 4498–4535. https://doi.org/10.1039/d0ee01355b.

Cheng, P., Chen, X., Gao, H., Zhang, X., Tang, Z., Li, A., and Wang, G. (2021). Different dimensional nanoadditives for thermal conductivity enhancement of phase change materials: fundamentals and applications. Nano Energy *85*, 105948. https://doi.org/10.1016/j.nanoen.2021.105948.

D'Oca, S., Hong, T., and Langevin, J. (2018). The human dimensions of energy use in buildings: a review. Renew. Sustain. Energy Rev. *81*, 731–742. https://doi.org/10.1016/j.rser.2017.08.019.

Hossain, M.M., and Gu, M. (2016). Radiative cooling: principles, progress, and potentials. Adv. Sci. *3*, 1500360. https://doi.org/10.1002/advs.201500360.

Hsu, P.C., Song, A.Y., Catrysse, P.B., Liu, C., Peng, Y., Xie, J., Fan, S., and Cui, Y.J.S. (2016). Radiative human body cooling by nanoporous polyethylene textile. Science *353*, 1019–1023. https://doi.org/10.1126/science.aaf5471.

Jaramillo-Fernandez, J., Whitworth, G.L., Pariente, J.A., Blanco, A., Garcia, P.D., Lopez, C., and Sotomayor-Torres, C.M. (2019). A self-assembled 2D thermofunctional material for radiative cooling. Small *15*, e1905290. https://doi.org/10.1002/smll.201905290.

Leroy, A., Bhatia, B.S., K Elsall, C.C., Castillejo-Cuberos, A., Di Capua H, M., Wang, E.N.J.S.A., Zhao, L., Zhang, L., Guzman, A.M., Wang, E.N., et al. (2019). High-performance subambient radiative cooling enabled by optically selective and thermally insulating polyethylene aerogel. Sci. Adv. *5*, eaat9480. https://doi.org/10.1126/sciadv.aat9480.

Li, D., Liu, X., Li, W., Lin, Z., Zhu, B., Li, Z., Li, J., Li, B., Fan, S., Xie, J., and Zhu, J. (2021). Scalable and hierarchically designed polymer film as a selective thermal emitter for high-performance all-day radiative cooling. Nat. Nanotechnol. *16*, 153–158. https://doi.org/10.1038/s41565-020-00800-4.

Li, T., Zhai, Y., He, S., Gan, W., Wei, Z., Heidarinejad, M., Dalgo, D., Mi, R., Zhao, X., Song, J., et al. (2019). A radiative cooling structural material. Science *364*, 760–763. https://doi.org/10.1126/science.aau9101.

Li, X., Peoples, J., Huang, Z., Zhao, Z., Qiu, J., and Ruan, X. (2020). Full Daytime Sub-ambient radiative cooling in commercial-like paints with high figure of merit. Cell Rep. Phys. Sci. *1*, 100221. https://doi.org/10.1016/j.xcrp.2020.100221.

Liang, S., Li, Q., Zhu, Y., Chen, K., Tian, C., Wang, J., and Bai, R. (2015). Nanoencapsulation of n-octadecane phase change material with silica shell through interfacial hydrolysis and polycondensation in miniemulsion. Energy *93*, 1684–1692. https://doi.org/10.1016/j.energy.2015.10.024.

Mandal, J., Fu, Y., Overvig, A.C., Jia, M., Sun, K., Shi, N.N., Zhou, H., Xiao, X., Yu, N., and Yang, Y.J.S. (2018). Hierarchically porous polymer coatings for highly efficient passive daytime radiative cooling. Science *362*, 315–319. https://doi.org/10.1126/science.aat9513.

Pakdel, E., Naebe, M., Sun, L., and Wang, X. (2019). Advanced functional fibrous materials for enhanced thermoregulating performance. ACS Appl. Mater. Interfaces *11*, 13039–13057. https://doi.org/10.1021/acsami.8b19067.

Pielichowska, K., and Pielichowski, K. (2014). Phase change materials for thermal energy storage. Prog. Mater. Sci. *65*, 67–123. https://doi.org/10.1016/j.pmatsci.2014.03.005.

Raman, A.P., Anoma, M.A., Zhu, L., Rephaeli, E., and Fan, S. (2014). Passive radiative cooling below ambient air temperature under direct sunlight. Nature *515*, 540–544. https://doi.org/10.1038/nature13883.

Rotzetter, A.C.C., Schumacher, C.M., Bubenhofer, S.B., Grass, R.N., Gerber, L.C., Zeltner, M., and Stark, W.J. (2012). Thermoresponsive polymer induced sweating surfaces as an efficient way to passively cool

buildings. Adv. Mater. *24*, 5352–5356. https://doi.org/10.1002/adma.201202574.

Shchukina, E.M., Graham, M., Zheng, Z., and Shchukin, D.G. (2018). Nanoencapsulation of phase change materials for advanced thermal energy storage systems. Chem. Soc. Rev. *47*, 4156–4175. https://doi.org/10.1039/c8cs00099a.

Shi, J., Huang, X., Guo, H., Shan, X., Xu, Z., Zhao, X., Sun, Z., Aftab, W., Qu, C., Yao, R., and Zou, R. (2020). Experimental investigation and numerical validation on the energy-saving performance of a passive phase change material floor for a real scale building. ES Energy Environ. *8*, 21–28. https://doi.org/10.30919/esee8c380.

Shi, J., Qin, M., Aftab, W., and Zou, R. (2021). Flexible phase change materials for thermal energy storage. Energy Storage Mater. *41*, 321–342. https://doi.org/10.1016/j.ensm.2021.05.048.

Wang, T., Wu, Y., Shi, L., Hu, X., Chen, M., and Wu, L. (2021). A structural polymer for highly efficient all-day passive radiative cooling. Nat. Commun. *12*, 365. https://doi.org/10.1038/s41467-020-20646-7.

Yuan, K., Shi, J., Aftab, W., Qin, M., Usman, A., Zhou, F., Lv, Y., Gao, S., and Zou, R. (2019). Engineering the thermal conductivity of functional phase-change materials for heat energy conversion, Storage, and Utilization. Adv. Funct. Mater. *30*, 1904228. https://doi.org/10.1002/adfm.201904228.

Liu, H., Zhu, S.N., Su, M., Wang, Z., and Tao, G.J.S. (2021). Hierarchical-morphology metafabric for scalable passive daytime radiative cooling. Science *66*, 3787–3790. https://doi.org/10.1360/tb-2021-0717.

Zhai, Y., Ma, Y., David, S.N., Zhao, D., Lou, R., Tan, G., Yang, R., and Yin, X.J.S. (2017). Scalable-manufactured randomized glass-polymer hybrid metamaterial for daytime radiative cooling. Science *355*, 1062–1066. https://doi.org/10.1126/science.aai7899.

Zhong, H., Li, Y., Zhang, P., Gao, S., Liu, B., Wang, Y., Meng, T., Zhou, Y., Hou, H., Xue, C., et al. (2021). Hierarchically hollow microfibers as a scalable and effective thermal insulating cooler for buildings. ACS Nano *15*, 10076–10083. https://doi.org/10.1021/acsnano.1c01814.

Zhou, D., Zhao, C.Y., and Tian, Y. (2012). Review on thermal energy storage with phase change materials (PCMs) in building applications. Appl. Energy *92*, 593–605. https://doi.org/10.1016/j.apenergy.2011.08.025.

Zhou, K., Li, W., Patel, B.B., Tao, R., Chang, Y., Fan, S., Diao, Y., and Cai, L. (2021). Three-dimensional printable nanoporous polymer matrix composites for daytime radiative cooling. Nano Lett. *21*, 1493–1499. https://doi.org/10.1021/acs.nanolett.0c04810.

## STAR★METHODS

### KEY RESOURCES TABLE

| REAGENT or RESOURCE | SOURCE | IDENTIFIER |
|---|---|---|
| Chemicals, peptides, and recombinant proteins | | |
| Octadecane | Honghu United Chemical Products Co., LTD. | Cas: 593-45-3 |
| Tetraethyl Orthosilicate (TEOS) | Yili Fine Chemicals Co. LTD. | Cas: 78-10-4 |
| Cetyltrimethyl Ammonium Bromide (CTAB) | Maclin | Cas: 57-09-0 |
| Acrylic Resin | Jincai New Material Co., LTD. | Cas: 25767-39-9 |

### RESOURCE AVAILABILITY

#### Lead contact

Further information and requests for resources and reagents should be directed to and will be fulfilled by the Lead Contact, Ruqiang Zou (rzou@pku.edu.cn).

#### Materials availability

This study did not generate new unique materials.

#### Data and code availability

All data reported in this article will be shared by the lead contact upon request.

This study does not report original code.

Any additional information required to analyze the data reported in this study is available from the lead contact upon request.

### METHOD DETAILS

#### Sample preparation

The octadecane@silica microcapsule is prepared through interfacial hydrolysis and polycondensation of TEOS in microemulsion with the existence of mixed water/ethanol solvents as continuous phase and melting paraffin as dispersed uniformly oil phase. The procedure refers to Liang's work with partly modified condition (Liang et al., 2015). In a typical experiment, the melted paraffin (10 g) is uniformly dispersed in TEOS (15 g) in a beaker (500 mL). And then the mixed deionized water (120 mL)/ethanol (90 mL) solvents and CTAB (2 g) are added into the beaker. The mixture is homogenized by the FSH-2A high speed homogenizer at the rate of 12000 rpm for 5 min and further by ultrasonic processor at the 50% power for 10 min to form a stable microemulsion. The microemulsion is transfer into a three necked flask and continually stirred by a mechanical stirrer at the rate of 300 rpm. Aqueous ammonia in the volume of 2.7 mL is added into the flask to initiate the reaction of interfacial hydrolysis and polycondensation of TEOS for 24 h. The octadecane@silica microcapsules are collected by suction filtration and washed with water, n-hexane and ethanol, then the samples were dried overnight in a vacuum oven at 50°C.

The composite paint is prepared as follow. The octadecane@silica microcapsules are mixed with ethanol firstly, followed by a 10-min stirring at the rate of 300 rpm to reduce particle agglomerations. The commercial acrylic resin is used as binder because of its alcohol dissolving and good IR emission capability. The acrylic resin is added into the mixture and was heat to 50°C to dissolve. To achieve high content of PCMs, the ratio of the microcapsule is up to 70%. The mixture was later painted to the substrate and dry 48 h at ambient temperature.

#### Morphologies and structure characterization of the microcapsules and paint

The morphologies of microcapsules and paint are investigated using a field emission scanning electron microscope (Hitachi, Regulus8220, Japan) under an acceleration voltage of 10 kV and a transmission electron

microscope (Philips-FEI, FEI Tecnai F30, Netherlands) with an EDS spectroscopy (Oxford instruments X-Max). The crystalline structure is determined in X-ray diffraction (XRD) patterns (PANalytical, X'Pert3 Powder, Netherlands) with Cu Kα radiation (λ = 0.15418 nm 40 kV 100 mA).

### Optical properties characterization of the microcapsules and paint

The real and imaginary part of the effective refraction index in sunlight spectrum region (0.25–2.5 μm) and in the mid-infrared wavelength ranges (2.5–25 μm) are determined in a spectral ellipsometry (Sentech, SE 850 DUV, Germany) and an infrared ellipsometer (Instruments GmbH, SENTECH, Germany), respectively. The spectral reflectance in the ultraviolet, visible and near-infrared (0.25–2.5 μm) wavelength ranges are determined in an UV-Vis-NIR spectrophotometer (Agilent Technologies, CARY5000, Malaysia) with a polytetrafluoroethylene integrating sphere and a polytetrafluoroethylene plane as standard reflecting pool. The average solar reflectance is calculated based on the AM 1.5 solar spectrum. The spectral emissivity in the mid-infrared wavelength ranges (2.5–25 μm) is characterized in an FTIR spectrometer (Bruker, VERTEX 80V, Germany) equipped with a gold integrating sphere.

### Thermal properties characterization of the microcapsules and paint

The phase change behaves of microcapsules and paint are characterized in a differential scanning calorimetry (DSC) (Netzsch, DSC 214 Polyma, Germany) under an Ar atmosphere with a temperature change rate of 5°C $min^{-1}$. The thermal stability is characterized in thermogravimetric analysis (TA Instruments, SDT Q600, America) with a heating rate of 10°C $min^{-1}$ under a $N_2$ gas flow. Thermal conductivity was characterized by laser thermal conductometer (NETZSCH, LFA467, America).

### The simulation of the scattering efficiency of microcapsule

The simulation is conducted with the FDTD Solution software (V8.6, Lumerical Solutions). For the simulation, the single core-shell particle with the diameter ratio of 0.8 and distribution from 500 nm to 1500 nm is constructed to simulate the microcapsule. PML boundary is used in three-dimensional cubic. The light source of TFSF with wavelength of 0.25–2.5 μm coupled with scattering space monitoring surface is used to calculate the scattering efficiency. The model is shown in Figure S3.

### Theoretical simplified model of the enhanced cooling performance

With incorporation of PCM and combining with radiative cooling model, the cooling power equation is expressed as: $P_{cooling}(T) = P_{rad}(T) - P_{atm}(T_{amb}) - P_{solar} - P_{cond+conv} + P_{phase}$ where $T$ is the temperature of the bifunctional paint and $T_{amb}$ is the ambient temperature. $P_{rad}(T)$ is the power radiated by bifunctional paint, and $P_{atm}(T_{amb})$ is the absorbed atmospheric thermal radiation at $T_{amb}$. $P_{solar}$ is the solar irradiation absorbed by the paint and $P_{cond+conv}$ is the power lost due to convection and conduction. $P_{phase}$ is the heat absorbed/released power by the phase transition, in the daytime it is positive value and nighttime negative. The simplified model calculated as: $P_{rad}(T) = \varepsilon_{paint}\sigma T_{paint}^{4}$, $P_{atm}(T_{amb}) = \varepsilon_{paint}\varepsilon_{air}\sigma T_{amb}^{4}$, $P_{solar} = (1-\rho)I_{AM1.5}$, $P_{cond+conv} = h(T_{amb} - T_{paint})$, $P_{phase} = m * H/t$. For this model, we only calculate the net cooling power for phase transition procedure with ideal PCMs whose melting point and freezing point are 28°C. The parameters for the equations are presented in the Table S1.